HANDOVER PARAMETER ADAPTATION BASED ON SINR REDUCTION RATE FOR 5G HETEROGENEOUS NETWORKS

Enrique R. Bastidas-Puga[1], Guillermo Galaviz[2], and Ángel G. Andrade[3]

Electrical Engineering Department, University of Baja California, Mexicali, Baja California, México
e-mail:[rbastidas[1], ggalaviz[2], aandrade[3]]@uabc.edu.mx

ABSTRACT

The use of highly dense heterogeneous networks (HetNet) to increase the network area capacity is a research topic for future 5G communication systems. Due to an increased probability of handover failures and handover ping-pongs in a HetNet, the handover procedure is particularly important to achieve seamless mobility. To reduce the probability of handover ping-pongs without increasing the probability of handover failures, in this work we propose a novel method to adapt the time to trigger and the handover margin based on the signal to interference plus noise ratio reduction rate. Numerical evaluations of the proposed method show lower overall handover failures and handover ping-pongs as compared to a handover procedure that uses fixed parameters.

1. INTRODUCTION

It is expected that over the next decade the number of devices connected to mobile-networks and their data rate requirements will continue to grow exponentially [1]. For instance, the number of network-connected wireless devices may reach 1000 times the world's population by 2017 [2]. To fulfill these requirements it is necessary to increase the spectral efficiency and network area capacity in terms of much higher per-user rate, which are some of the main drivers behind the future development of 5G communications systems.

The spectral efficiency can be increased with technologies like massive multiple input multiple-output (MIMO), cognitive radio or spectrum sharing by using the same spectral resources. On the other hand, increasing the network area capacity to support the mobile data traffic growing trend, will require the deployment of more small-cells (picocells or femtocells) per area unit [1].

This heterogeneity of the 5G cellular architecture which, consist of macrocells highly densified by small-cells using the same radio access technology (RAT), will allow more efficient spectrum reuse and therefore larger data rates [2]. However, as 5G networks become progressively denser and heterogeneous, the user equipment (UE) mobility management will be more challenging, since the network will have decide on switching the UE's connection-channel, whenever a UE moves into a small-cell from macrocell, or moves out of a small-cell.

In mobile-communication networks the UE mobility is supported by the handover procedure. A handover is the connection transfer of a UE, from a source node to a target node, in order to maintain communication with a specific quality of service (QoS) [3]. Different conditions between the UE and a source node trigger a handover, such as: a reduction of the received power when the UE moves from a serving node to another, fluctuations of the received power from the source node and a neighbor node, or a radio link quality reduction, measured in terms of signal-to-interference noise ratio (SINR), due to an increase of the received interference.

During the handover procedure, a handover failure (HOF) occurs if the SINR from the source node falls below a threshold before the completion of the handover, thus interrupting the connection [3], [4]. Such interruption also causes the consumption of additional network resources, since the network needs to start connection-recovery procedures thereafter.

The preparation and execution of the handover procedure involves a series of steps in which control signals and user data are exchanged between the UE, the source node, and the target node. This exchange of signaling information consumes network resources. When there is a connection transfer in the network, a handover ping-pong (HOPP) is produced if the UE connects to a new node, and in a very short period of time completes a handover back to its former source node [3], [4]. In general the HOPPs may be considered as handovers that if avoided, the network resources employed for the connection transfer procedure could be saved.

As reported in recent works, HOFs and HOPPs affect the mobility management performance of heterogeneous networks (HetNets) to a greater extent than macrocells-only networks [4]. QoS has always been an important aspect of network design to provide an adequate user experience. Also, network resources such as time, spectrum and power are limited and need to be managed efficiently to maximize their use. Given these conditions, there is a need for strategies that reduce the occurrence of HOFs and HOPPs that deteriorate the QoS and consume additional network resources, particularly in HetNets.

A UE that moves away from its source node suffers a reduction of the received power due to the signal path loss, while most likely, the interference increases since the UE gets closer to other nodes. Therefore it is expected that the SINR gets reduced over time.

One factor that affects the occurrence of an HOF and an HOPP is the connection transfer starting time (CTST) within the handover process. If there is an advance of the CTST, then the handover completes earlier. Therefore, an advanced CTST will reduce the probability of the SINR to drop below a required threshold before completing the handover, preventing an HOF. However, it will increase the probability of an HOPP, as the handover might be performed with no need. The opposite happens with a delayed CTST.

The handover time to trigger (TTT) and the handover margin (HOM) are two parameters of the handover procedure that control the CTST [3], [4]. Typical handover procedures make use of constant values of TTT and HOM, which are selected based on a tradeoff between the HOF rate (HOFR) and the HOPP rate (HOPR) [3].

One way of reducing the probability of HOF and HOPP is to adapt handover parameters that control the CTST. The idea of adapting handover parameters is presented in works like [5], [6], and [7]. In [5] the handover parameters are selected according to the type of nodes involved in the connection transfer, while the proposals in [6] and [7] rely on performance metrics tracking to adapt handover parameters.

Knowledge of the SINR variation rate can be used to determine the latest possible CTST without causing an HOF. A late CTST allows to reduce the probability of an HOPP. The SINR reduction rate provides key information to determine the time at which the SINR falls below a threshold that produces an HOF, making it possible to consider the SINR reduction rate as a decision variable to adapt the CTST.

In this paper we propose a method to adapt TTT and HOM based on the SINR reduction rate. As a result, the CTST is adapted according to the link condition of each UE, thus reducing the probability of HOPP without increasing the probability of HOF. To achieve this, the SINR measurements that each UE utilize to report a channel quality indicator (CQI) to the source node are used. Numerical evaluations of our proposal show that the reduction of HOFR and HOPR is significant as compared to a handover procedure with fixed TTT and HOM.

The rest of this paper is organized as follows: Section 2 presents the system model. The proposed method of adaptable handover parameters (AHP) is described in Section 3. The description of the evaluation for the AHP method is presented in Section 4. Section 5 shows the numerical analysis of results obtained by simulations, and finally Section 6 includes the conclusions.

2. SYSTEM MODEL

LTE-Advanced systems make use of hard handover techniques. This implies that the UE is first disconnected from its source evolved node (eNB), or base station, and after some time (in the milliseconds order) it establishes a new connection with a target eNB [8].

The UE reports to its source eNB the reference signal received power ($RSRP$) from neighbor eNBs. In [9] the $RSRP$ is defined as the linear average of the power contributions (in watts) of the resource elements that carry cell-specific reference signals within a considered measurement bandwidth.

The source eNB initiates a handover if an event known as A3 is active during a period of TTT seconds [10]. The event A3 activates if the $RSRP$ from a target eNB ($RSRP_t$) is larger than the $RSRP$ from the source eNB ($RSRP_s$) plus two decision offsets: HOM and hysteresis (HYS) [10]. The TTT timer initializes upon the event A3 entry condition which is shown in (1), where $RSRP_t$ and $RSRP_s$ are given in decibel-milliwatts (dBm), while HOM and HYS are given in decibels (dB).

$$RSRP_t > RSRP_s + HOM + HYS. \tag{1}$$

On the other hand, the event A3 deactivates if the condition (2) is met before the TTT expires, which prevents handover from starting [10].

$$RSRP_t < RSRP_s + HOM - HYS. \tag{2}$$

In (1) we can see that HOM and HYS add up to specify the power offset between $RSRP_t$ and $RSRP_s$ for the event A3 entry condition, which in a practical sense is equivalent to a single offset.

In this paper we are interested in the CTST, which is partially determined by the event A3 entry condition. The A3 entry condition is in turn determined by the power offset ($HOM+HYS$). For simplicity we consider HYS equal to zero, therefore the power offset is solely determined by HOM.

The handover procedure can be divided in two stages: the handover preparation stage and the handover execution stage. The handover preparation stage initiates once the source eNB starts the handover; it includes the handover request from source eNB to target eNB; the target eNB admission control procedure, which accepts or rejects the handover request based on resources availability; the handover request acknowledgment from target eNB to source eNB; and finally the handover command from source eNB to UE, i.e., the instruction to connect to target eNB [8]. Figure 1 shows the handover steps.

During the handover execution stage, the UE disconnects from its source eNB, synchronizes to target eNB, and gains access to it through a random access channel (RACH) following a contention-free procedure if a dedicated RACH preamble was indicated by the target eNB with the handover request acknowledgment, or a contention-based procedure if no dedicated RACH preamble was indicated; then the target eNB responds with uplink (UL) allocation; and finally, the UE sends a radio resource control connection reconfiguration complete message (RRC_crc_msg) to target eNB [8]. At this point the handover procedure is complete from the UE tasks perspective.

Figure 2 shows a time chart of the handover stages: t_0 is a reference time indicating the moment at which $RSRP_t$ is equal to $RSRP_s$; t_1 marks the time at which the event A3 entry condition is met and thus the TTT timer initializes; t_2 is the time

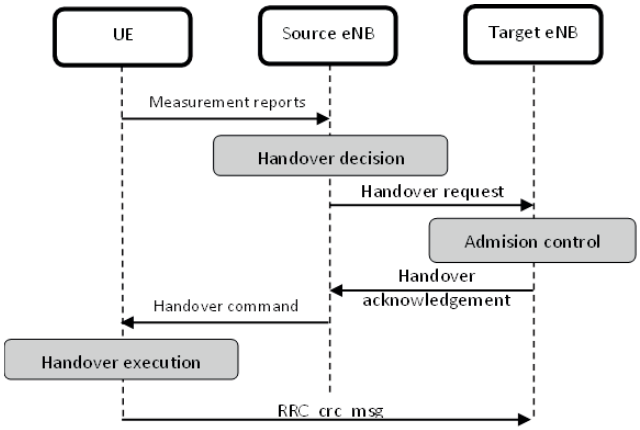

Figure 1: Handover procedure.

when source eNB decides to initiate the handover (the CTST) if the event A3 is active when TTT timer expires. Let T_{HOp} and T_{HOe} be the time taken by the network for the handover preparation and execution stages respectively. Finally, t_4 is the instant at which the UE connection to target eNB is complete.

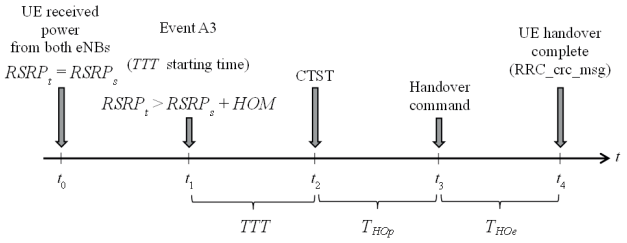

Figure 2: Handover time chart.

The parameters HOM and TTT control the CTST. The HOM advances or delays the CTST by shifting t_1 from t_0 in Fig. 2, while TTT advances or delays the CTST by shifting t_2 from t_1.

2.1. Handover Failure

During the handover process, a radio link failure (RLF) may cause an HOF. An HOF is declared if any of the following conditions is met [4]:

1. $SINR$ from source eNB ($SINR_s$) is less than an $SINR_{out}$ threshold when the handover command is sent to the UE (t_3 in Fig. 2).

2. An RLF is declared anytime between the TTT starting time and sending the handover command to UE (between t_1 and t_3 in Fig. 2). The RLF is declared if the $SINR_s$ is less than $SINR_{out}$ during $T310$ seconds. The timer $T310$ is defined in 3GPP specifications in order to track down RLFs [10].

3. $SINR$ from target eNB ($SINR_t$) is less than $SINR_{out}$ when the RRC_crc_msg is sent (t_4 in Fig. 2).

Since an HOF is determined by the $SINR_s$, then the $SINR_s$ reduction rate provides key information to prevent HOFs.

If the $SINR_s$ reduction rate is high, then the mobile network has less time to successfully complete the handover, and viceversa. Adapting HOM and TTT allows the network to modify the CTST by shifting t_1 and t_2 to advance or delay the handover as required.

2.2. Handover Ping-Pong

HOPPs are determined by the time of stay (ToS), which is the time that a UE stays connected with a node after a handover. The ToS is measured from the moment the UE sends the RRC_crc_msg to a target eNB (t_4 in Fig. 2) until the UE sends a new RRC_crc_msg to another target eNB [4].

An HOPP is declared if a UE completes a handover from eNB-A to eNB-B, and connects back from eNB-B to eNB-A given a ToS in eNB-B less than a minimum time of stay (MTS) [4]. The MTS is altogether specified by the time that a UE needs to establish a reliable connection with the eNB and the required time for conducting efficient data transmission [4].

If the ToS is less than the MTS, the connection transfer may be considered as an unnecessary handover that increments the control signaling and consumes network resources.

One factor that produces HOPPs is the fluctuation of $RSRP_s$ and $RSRP_t$ due to fading. Waiting a longer time to initiate the handover allows the network to deactivate the event A3 if the received power variations are due to temporal fluctuations. This can prevent the handover from starting and reduces the probability of HOPPs. The CTST can be delayed with larger HOM and TTT at the cost of increasing the probability of HOFs because the handover is delayed.

Therefore we propose to adapt HOM and TTT according to the SINR reduction rate, in order to delay the CTST as much as possible, to reduce the probability of HOPP without increasing the probability of HOF caused by connection failure with source eNB.

3. ADAPTABLE HANDOVER PARAMETERS METHOD

With the purpose of adapting the TTT and HOM to provide the latest possible CTST that reduces the probability of HOPP without increasing the probability of HOF, an AHP method is proposed. One important aspect of the proposed AHP method is the ability to anticipate if an HOF will be produced or not for a link quality condition and a determined CTST. Let us define the link quality condition of a UE with its source node, as the $SINR_s$ and its corresponding $SINR_s$ reduction rate.

In case of handover, if the link quality condition at a given time t_0 is known (see Fig. 2), then it can be used together with a prediction model to estimate the $SINR_s$ at a later time

t_3 [$SINR_s(t_3)$]. An HOF can be anticipated if the predicted $SINR_s(t_3)$ is less than $SINR_{out}$. To prevent an HOF, the CTST can be modified as needed by adapting the HOM and the TTT, in such a way that the $SINR_s(t_3)$ turns out to be a desired $SINR_{des}(t_3) > SINR_{out}$.

Our proposal is to adapt HOM and TTT at t_0 (see Fig. 2) for each user according to its link quality condition.

In LTE systems the UE periodically estimates $SINR_s$ to report a CQI to its source eNB, therefore the $SINR_s$ estimation performed by the UE can be used to estimate the $SINR_s$ reduction rate.

In practice, UEs in LTE systems estimate the $SINR$ considering the ratio between the RSRP and the received signal strength indicator (RSSI) times the number of resource blocks for the corresponding bandwidth [9]. The RSSI is the linear average of the total received power including interference and thermal noise in a given measurement bandwidth [9].

Once the $SINR_s$ reduction rate is estimated, the AHP method advances the CTST for high $SINR_s$ reduction rates by adapting small HOM and TTT values, or delays the CTST for low $SINR_s$ reduction rates by adapting large HOM and TTT values. Figure 3 presents the block diagram of the AHP method operations.

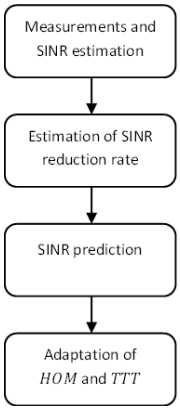

Figure 3: AHP method operations.

3.1. Prediction model

The AHP method makes use of a model to predict $SINR_s(t_3)$ given a link quality condition at t_0. With the prediction model, the HOM and TTT are adapted for a desired value of $SINR_{des}(t_3)$ in order to avoid an HOF.

In this work, we use the truncated Taylor Series (linear approximation) of $SINR_s(t_3)$ in (3) as a prediction model [11].

$$SINR_s(t_3) \approx SINR_s(t_0) + [SINR'_s(t_0)](t_3 - t_0). \quad (3)$$

In (3), $SINR'_s(t_0) = \frac{d[SINR_s(t_0)]}{dt}$ is the $SINR_s$ change rate (negative of reduction rate) at time t_0, and $(t_3 - t_0)$ is obtained with (4), where $(t_1 - t_0)$ can be approximated with (5).

$$(t_3 - t_0) = (t_1 - t_0) + TTT + T_{HOp}. \quad (4)$$

$$(t_1 - t_0) \approx \frac{HOM}{\frac{d[RSRP_t(t_0)]}{dt} - \frac{d[RSRP_s(t_0)]}{dt}}. \quad (5)$$

We define a configuration parameter named time ratio (TR) in (6) that allows the network operator to establish a ratio between the elapsed time since $RSRP_t$ equals $RSRP_s$ until the event A3 entry condition, and the elapsed time since the event A3 entry condition until the CTST (see Fig. 2).

$$TR = \frac{t_1 - t_0}{TTT}. \quad (6)$$

Therefore, we can solve TTT from (3), (4), and (6) to obtain (7), while HOM can be solved from (5) and (6) to obtain (8).

$$TTT = \frac{1}{TR+1} \cdot \left(\frac{SINR_{des}(t_3) - SINR_s(t_0)}{\frac{d[SINR_s(t_0)]}{dt}} - T_{HOp} \right) \quad (7)$$

$$HOM = TTT \cdot TR \cdot \left(\frac{d[RSRP_t(t_0)]}{dt} - \frac{d[RSRP_s(t_0)]}{dt} \right) \quad (8)$$

With (7) and (8), TTT and HOM can be adapted at time t_0 to approximate a desired $SINR_{des}(t_3)$ value that prevents the HOF. For a given $SINR_{des}(t_3) > SINR_{out}$ the CTST will occur later as the $SINR_{des}(t_3)$ is set closer to $SINR_{out}$, therefore reducing the HOPP probability.

In this paper we focus on the TTT and HOM adaptation according to the $SINR_s$ reduction rate rather than on the estimation of the reduction rate.

Since $\frac{d[SINR_s(t_0)]}{dt}$, $\frac{d[RSRP_s(t_0)]}{dt}$, and $\frac{d[RSRP_t(t_0)]}{dt}$ are needed for (7) and (8), we implemented a logarithmic curve fitting with up to N corresponding measurements taken by the UE ($SINR_s$, $RSRP_s$, or $RSRP_t$) and then estimated the respective change rate with finite differences [11]. With (9) we can estimate the $SINR_s$ change rate at time t_0, where t_{-1} is the instant of the measurement taken by the UE previous to t_0. $\frac{d[RSRP_s(t_0)]}{dt}$ and $\frac{d[RSRP_t(t_0)]}{dt}$ can also be estimated with finite differences of their respective fitted values measurements.

$$\frac{d[SINR_s(t_0)]}{dt} \approx \frac{SINR_s(t_0)_{fitted} - SINR_s(t_{-1})_{fitted}}{t_0 - t_{-1}}. \quad (9)$$

4. EVALUATION

The evaluation of the proposed AHP method was performed by comparing the HOFR and the HOPR of a system that uses a

handover procedure with constant values of HOM and TTT against a system that uses the AHP proposal.

The HOFR and the HOPR were obtained through Monte Carlo simulation of a system with mobile UEs requiring handovers. The HOFR and the HOPR are defined in (10) and (11) respectively, where $nHOF$ is the number of HOFs, $nAHO$ is the number of attempted handovers, $nHOPP$ is the number of HOPPs, and nHO is the number of successfully completed handovers.

$$HOFR(\%) = \frac{nHOF}{nAHO} \times 100. \quad (10)$$

$$HOPR(\%) = \frac{nHOPP}{nHO} \times 100. \quad (11)$$

Since the AHP method was developed to advance the CTST for large $SINR_s$ reduction rates and to delay the CTST for small $SINR_s$ reduction rates, the evaluation of the HOFR and HOPR was done to capture the results with a wide range of $SINR_s$ reduction rates, which was accomplished by considering UEs moving from low to high velocities.

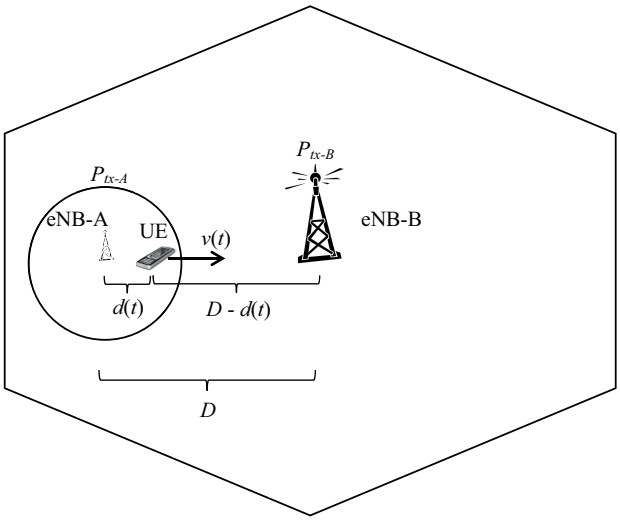

Figure 4: Picocel to macrocell handover scenario.

Figure 4 shows the evaluation scenario with a UE in a picocell (eNB-A) service area moving towards a macrocell (eNB-B) in straight trajectory with constant velocity $v(t)$. The UE requires a picocell to macrocell handover. The eNB-A to eNB-B distance is D, and the UE to eNB-A distance at time t is $d(t)$. The picocell and macrocell transmission powers are P_{tx-A} and P_{tx-B} respectively.

For each UE in movement, the simulation obtains the $RSRP_s$ and the $RSRP_t$ with the respective eNB transmission power and the path loss (PL) model for a cellular urban line of sight (LOS) scenario (12) [12], where PL is in decibels, f_c is the carrier frequency in gigahertz, and X is a normal random variable of the fading effect with 0 dB mean and standard deviation σ in decibels. Then the $RSRP_s$ and $RSRP_t$ are used together with the HOM and the TTT values to determine the times of the handover stages (see Fig. 1) in order to keep track of the $nAHO$, nHO, $nHOF$, and $nHOPP$.

$$PL[d(t)] = 22\log_{10}[d(t)] + 28 + 20\log_{10}(f_c) + X. \quad (12)$$

The interference is considered with a random variable for the $SINR_s$ at time t_0 and the variation of the $SINR_s(t)$ for any other time is determined by the $RSRP_s$ fluctuations due to the PL model with fading effects and the UE velocity.

It was considered that the target eNB always had resources to accept the handover. This consideration was done because if an HOF is produced due to the lack of resources in the target eNB, it affects the same way whether the handover procedure uses constant HOM and TTT or the AHP method.

The scenario described in Fig. 4 is simple, but it includes a wide range of UE link quality conditions to evaluate the performance of the proposed AHP method in terms of HOFR and HOPR. In the evaluation, the link quality conditions are determined by the variations of the RSRP due to the PL model with fading effects and the UE velocities.

5. ANALYSIS OF NUMERICAL RESULTS

In this section we present results of adapted TTT and HOM based on numerical evaluations of (7) and (8). We also present results of HOFR and HOPR based on simulations for a system that uses a handover procedure with constant TTT and HOM and for a system that uses the proposed AHP method. The simulations considered the evaluation scenario described in last section with the parameter settings shown in Table 1.

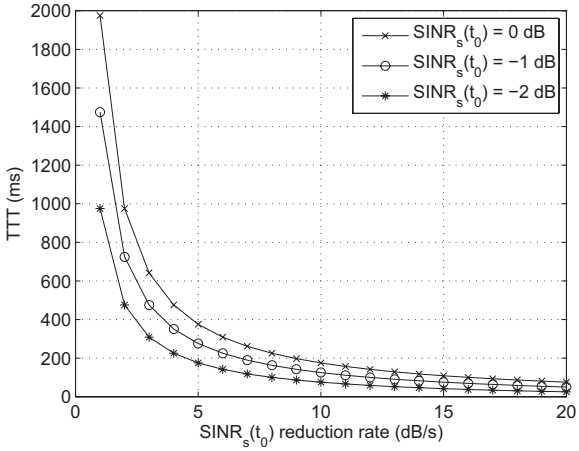

Figure 5: Adapted TTT.

Figures 5 and 6 show results of the adapted TTT and HOM for different link quality conditions of the UE at t_0 respectively.

The TTT and HOM were obtained with (7) and (8) for an $SINR_{des}(t_3) = -4$ dB and $\frac{d[RSRP_t(t_0)]}{dt} = -4$ dB/s. Since

Table 1: Simulation settings

Parameter	**Value**
Path loss model	Urban macro-cellular LOS
Fading model	Log-normal shadow fading
Fading standard deviation (σ)	4 (dB)
Fading correlation distance (d_{corr})	25 (m)
Source eNB to target eNB distance (D)	200 (m)
UE velocity [$v(t)$]	[3,10,30,60,100,120] (km/h)
eNB-A transmission power (P_{tx-A})	30 (dBm)
eNB-B transmission power (P_{tx-B})	46 (dBm)
Frequency (f_c)	2 (GHz)
UE measurement period	10 (ms)
Minimum time of stay (MTS)	2 (s)
RLF threshold ($SINR_{out}$)	-8 (dB)
RLF timer ($T310$)	1 (s)
$SINR_s(t_0)$	$\sim U[-3, 0]$ (dB)
Handover preparation time (T_{HOp})	50 (ms)
Handover execution time (T_{HOe})	40 (ms)
Time ratio (TR)	1
Time to trigger (TTT)	[40, 240, 440, 640] (ms)
Handover margin (HOM)	[1, 2, 3, 4] (dB)

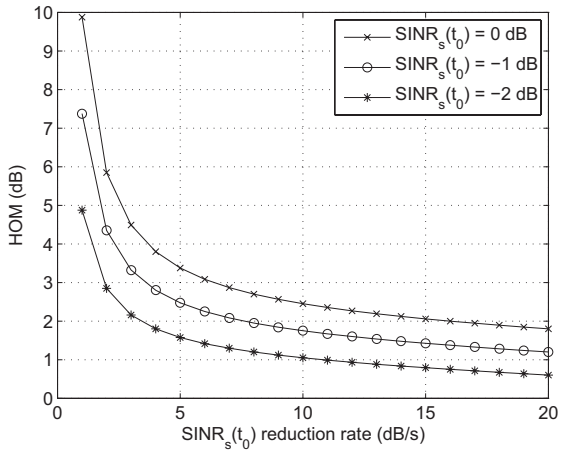

Figure 6: Adapted HOM.

the purpose of data in Figs. 5 and 6 is to show how the AHP method adapts TTT and HOM for different $SINR_s$ reduction rates and $SINR_s(t_0)$, we considered for simplicity of this particular numerical evaluation that the $RSRP_s$ reduction rate was equal to the $SINR_s$ reduction rate.

Data in Figs. 5 and 6 confirm that the AHP method achieves its purpose to adapt large TTT and HOM values for small $SINR_s$ reduction rates, thus the CTST is delayed, while it adapts small TTT and HOM values for large $SINR_s$ reduction rates, therefore the CTST is advanced.

Results in Figs. 5 and 6 also indicate that for equal $SINR_s$ reduction rate and different $SINR_s(t_0)$, if the $SINR_s(t_0)$ is smaller then the AHP method adapts smaller TTT and HOM values too, i.e., it advances the CTST because the $SINR_s$ is closer to the RLF threshold $SINR_{out}$.

5.1. Results with constant HOM and TTT

The evaluation of HOFR and HOPR was first performed with simulations of a system that uses constant TTT and HOM. The metrics were estimated with (10), (11), and the method of batch means, [13], for $M = 4$ simulation runs with $n = 36000$ UEs in movement (6000 for each velocity in Table 1).

Table 2: HOFR (%) and 95% CI

	TTT**(ms)**			
HOM**(dB)**	40	240	440	640
1	4.11	12.81	22.02	28.97
	4.00-4.22	12.52-13.10	21.59-22.46	28.60-29.33
2	6.49	18.52	28.07	35.18
	6.38-6.60	18.27-18.77	27.82-28.33	35.04-35.32
3	10.09	25.14	34.66	41.04
	9.84-10.33	24.63-25.66	34.36-34.96	40.56-41.53
4	15.74	32.47	41.77	47.59
	15.41-16.06	32.18-32.76	41.49-42.05	46.89-48.28

Table 3: HOPR (%) and 95% CI

	TTT**(ms)**			
HOM**(dB)**	40	240	440	640
1	27.75	6.46	2.34	1.10
	26.90-28.60	6.13-6.81	2.20-2.49	0.96-1.24
2	9.34	1.24	0.31	0.10
	9.00-9.68	1.14-1.34	0.23-0.39	0.07-0.14
3	2.68	0.24	0.03	0.01
	2.39-2.96	0.18-0.30	0.00-0.07	0.00-0.02
4	0.67	0.04	0.00	0.00
	0.58-0.76	0.02-0.06	0.00-0.01	0.00-0.00

Tables 2 and 3 present the HOFR and HOPR results with their respective 95% confidence intervals (CI) for a system with constant TTT and HOM. The CIs are presented to give an idea of the precision and the confidence level of the HOFR and HOPR estimation.

In Table 2, the best case of HOFR (4.11%) is achieved with a $TTT = 40$ ms and an $HOM = 1$ dB, but at the same time it corresponds to the worst case of HOPR (27.75%) as shown in Table 3. The data also indicate that increasing TTT and/or HOM (delaying the CTST) reduces the HOPR but increases the HOFR, which confirms the tradeoff between HOPR and HOFR as shown in [3].

Figure 7 indicates that the HOFR is less sensitive to changes of HOM than to changes of TTT. The chart shows the resulting HOFR change (ΔHOFR) to achieve a determined HOPR change (ΔHOPR) with respect to the reference setting $HOM = 1$ dB and $TTT = 40$ ms from Tables 2 and 3. In the figure we can

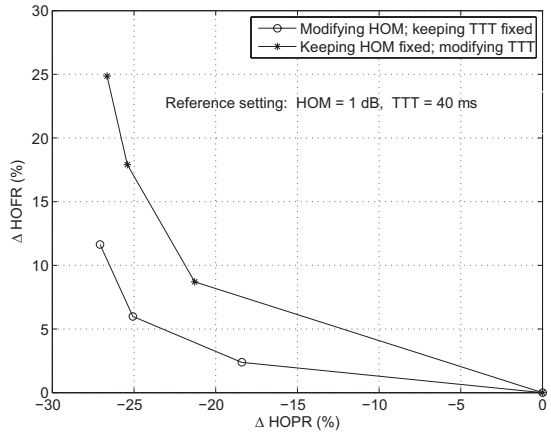

Figure 7: HOFR sensitivity to changes of HOM and TTT.

see that for reducing a given value of HOPR (from 27.75%), the HOFR increment is smaller if only the HOM is changed as compared to if only the TTT is changed.

The difference in the sensitivity of the HOFR to changes of HOM as compared to the changes of TTT can be explained by their measure units. The HOF is determined by the $SINR_s$ and the $SINR_{out}$ threshold, both in logarithmic scale (decibels) as it is the case of the HOM, but the TTT units are linear. This finding may lead to a variant of the AHP method for which the TTT is kept constant and only the HOM is adapted.

5.2. Results with AHP method

For the AHP proposal, the HOFR and the HOPR were also evaluated using (10), (11), and the method of batch means, with $M = 4$ simulation runs and $n = 36000$ UEs in movement. All the parameters settings were the same (see Table 1) but the HOM and TTT were adapted with (7) and (8).

Table 4 shows the HOFR, the HOPR, and the respective CIs for a system that uses the AHP method considering a desired $SINR_{des}(t_3) = -3.0$ dB.

Table 4: HOFR, HOPR, and 95% CI for the AHP method.

HOFR(%)	5.89
	5.66-6.12
HOPR(%)	5.99
	5.84-6.15

For the AHP method, the HOFR is 5.89% with an HOPR of 5.99%, while for the handover procedure with constant HOM and TTT the best case of HOFR is 4.11% with an HOPR of 27.75% (Tables 2 and 3). In the case of the AHP method the HOFR slightly increases while the HOPR decreases considerably.

From Tables 2 and 3 we can see that a close value to the 5.99% HOPR of the AHP method can be achieved with $HOM = 1$ dB and $TTT = 240$ ms, resulting in an HOPR of 6.46% but with an HOFR of 12.81%, which is larger than the corresponding HOFR of 5.89% from the AHP method.

Therefore these data indicate that when comparing the AHP method with the handover procedure that uses constant HOM and TTT, if both HOFRs are close then the HOPR is smaller for the AHP method, or if both HOPRs are close, then the HOFR is smaller for the AHP method.

Even though the AHP method performs better than the handover procedure with constant HOM and TTT, we can see that the HOFs were not avoided with the desired $SINR_{des}(t_3)$ of -3.0 dB, which is larger than the $SINR_{out}$ threshold of -8 dB. This could be related to the prediction model in (3).

An advantage of the prediction model (3) is that it is linear, so it only needs the $SINR_s(t_0)$ value and the $SINR_s(t_0)$ reduction rate to be implemented (the link quality condition), but at the same time its linearity is a drawback, because it considers that the $SINR_s$ reduction rate remains constant to predict the $SINR_s(t_3)$. In practice the $SINR_s$ reduction rate varies over time as it depends on the distance from the UE to the source node, which is changing since the UE is in movement. So a different prediction model could improve the accuracy of the predicted $SINR_s(t_3)$ to reduce even further the HOFR and the HOPR.

6. CONCLUSIONS

We have proposed a method that adapts the time to trigger and handover margin to improve the performance of the handover procedure in terms of the HOFR and the HOPR in HetNets. The method adapts the HOM and TTT according to the $SINR_s$ reduction rate. Numerical results show the potential of the method to reduce HOFR and HOPR as compared to a handover procedure that uses constant HOM and TTT. Future work in this research could consider an alternative SINR prediction model to improve the results even further, such as a higher order truncated Taylor series, or a logarithmic model.

REFERENCES

[1] J. Andrews, S. Buzzi, W. Choi, S. Hanly, A. Lozano, A. Soong, and J. Zhang, "What will 5G be?" *Selected Areas in Communications, IEEE Journal on*, vol. 32, no. 6, pp. 1065–1082, June 2014.

[2] W. Cheng-Xiang, F. Haider, G. Xiqi, Y. Xiao-Hu, Y. Yang, Y. Dongfeng, H. Aggoune, H. Haas, S. Fletcher, and E. Hepsaydir, "Cellular architecture and key technologies for 5G wireless communication networks," *Communications Magazine, IEEE*, vol. 52, no. 2, pp. 122–130, February 2014.

[3] D. Lopez-Perez, I. Guvenc, and X.Chu, "Mobility management challenges in 3GPP heterogeneous networks," *Communications Magazine, IEEE*, vol. 50, no. 12, pp. 70–78, 2012.

[4] 3GPP, "Mobility Enhancements in Heterogeneous Networks," 3GPP, Technical Report TS 36.839 v11.1.0, December 2012.

[5] W. Gao, B. Jiao, G. Yang, W. Hu, L. Chi, and J. Liu, "Mobility robustness improvement through transport parameter optimization in HetNets," in *Personal, Indoor and Mobile Radio Communications (PIMRC Workshops), 2013 IEEE 24th International Symposium on*, 2013, pp. 101–105.

[6] P. Munoz, R. Barco, and I. de la Bandera, "On the Potential of Handover Parameter Optimization for Self-Organizing Networks," *Vehicular Technology, IEEE Transactions on*, vol. 62, no. 5, pp. 1895–1905, 2013.

[7] T. Jansen, I. Balan, S. Stefanski, I. Moerman, and T. Kurner, "Weighted Performance Based Handover Parameter Optimization in LTE," in *Vehicular Technology Conference (VTC Spring), 2011 IEEE 73rd*, 2011, pp. 1–5.

[8] 3GPP, "Technical Specification Group Radio Access Network; Evolved Universal Terrestrial Radio Access (E-UTRA); Overall description; Stage 2 (Release 11)," 3GPP, Technical Specification TS 36.300 v11.3.0, 2012.

[9] 3GPP, "Technical Specification Group Radio Access Network; Evolved Universal Terrestrial Radio Access (E-UTRA); Physical layer measurements (Release 11)," 3GPP, Technical Specification TS 36.214 V11.1.0, 2012.

[10] 3GPP, "Radio Resource Control (RCC); Protocol Specification (Release 11)," 3GPP, Technical Specification TS 36.331 V11.6.0, 2013.

[11] S. Chapra and R. Canale, *Numerical Methods for Engineers*, 6th ed. McGraw-Hill, 2009.

[12] ITU, "Guidelines for Evaluation of Radio Interface Technologies for IMT-Advanced," ITU-R, Technical Report ITU-R M.2135, 2008.

[13] A. Leon-Garcia, *Probability and Random Processes for Electrical Engineering*, 2nd ed. Addison-Wesley, 1994.